Proceedings of IPACK2005
ASME InterPACK '05
July 17-22, San Francisco, California, USA

IPACK2005-73181

ORTHOTROPIC THERMAL CONDUCTIVITY EFFECT ON CYLINDRICAL PIN FIN HEAT TRANSFER

Raj Bahadur, Avram Bar-Cohen
Department of Mechanical Engineering, University of Maryland,
College park, MD 20742, USA

ABSTRACT

There is growing interest in the use of polymer composites with enhanced thermal conductivity for high performance fin arrays and heat sinks. However, the thermal conductivity of these materials is relatively low compared to conventional fin metals, and strongly orthotropic. Therefore, the design and optimization of such polymer pin fins requires extension of the one dimensional classical fin analysis to include two-dimensional orthotropic heat conduction effects.

An analytical equation for heat transfer from a cylindrical pin fin with orthotropic thermal conductivity is derived and validated using detailed finite-element results. The thermal performance of such fins was found to be dominated by the axial thermal conductivity, but to depart from the classical fin solution with increasing values of a radius- and radial conductivity-based Biot number. Using these relations, it is determined that fin orthotropy does not materially affect the behavior of typical air-cooled fins. Alternatively, for heat transfer coefficients achievable with water cooling and conductivity ratios below 0.1, the fin heat transfer rate can fall more than 25% below the "classical" heat transfer rates. Detailed orthotropic fin temperature distributions are used to explain this discrepancy. Simplified orthotropic pin fin heat transfer equations are derived and validated over a wide range of orthotropic conditions.

KEYWORDS

Orthotropic thermal conductivity, Biot number, pin fin heat transfer, polymer composites, carbon fiber, fin optimization, heat sink.

INTRODUCTION

Recent advances in polymer composites, using carbon fiber, [1], and graphite fillers, [2], to increase the thermal conductivity, have made such materials viable alternatives to conventional metals in the design and fabrication of heat sinks and heat exchangers [see in Table 1]. Ongoing research into the use of carbon nano tubes (CNT's), [3], in epoxy matrixes may yield further improvements in such polymer composites. In addition to the manufacturing advantages offered by such moldable, high thermal conductivity composites, their relatively low density can provide a significant weight reduction and require less energy for formation and fabrication than copper and aluminum – yielding an important contribution to sustainability [4].

Table 1: Polymer composite properties

Filler	Matrix	Parallel to fibers (W/m-K)	Normal to fibers (W/m-K)	Density (g/cc)	Wt (%) filler
Continuous carbon fiber	Polymer	330 [1]	3-10	1.8	NA
Discontinuous carbon fiber	Polymer	10-100 [1]	3-10	1.7	NA
Graphite	Epoxy	370 [2]	6.5	1.94	NA
Single walled nanotubes	Epoxy	0.5 [3]	NA	NA	1
Thermal graph DKD X	Lexan HF 1110-11N	8.0 [20]	0.6	1.38	30
Thermal graph DKD X	Lexan HF 1110-11N	11.4 [20]	0.74	1.46	40
Thermocarb CF-300	Zytel 101 NC010	1.1[20]	0.4	1.17	5
Thermocarb CF-300	Zytel 101 NC010	4.4 [20]	0.8	1.33	30

Conventional polymers can be expected to display thermal conductivities in the range of 0.15-0.5W/mK, but with the addition of high thermal conductivity continuous carbon fibers these composites can reach thermal conductivities of 300W/mK in the fiber axis direction, as shown in Table 1. They display far lower thermal conductivities in the orthogonal (perpendicular to fiber axis) direction, with values that are 2 orders of magnitude lower, i.e. 3 W/m-K The pitch based discontinuous fibers results in axial conductivity up to 100 W/m-K and radial conductivity as low as the polymer conductivity of 0.4 W/m-K. The impact of this orthotropy on the accuracy of classical one-dimensional thermal performance predictions for polymer composite single fins and fin arrays has yet to be established. Failure to properly account for the role of orthotropy could limit the thermal designer's ability to predict and optimize the thermal performance of such polymer composite fins and heat

sinks. It will also severely compromise any attempt at a thermo-mechanical optimization for achieving superior thermal performance with acceptable mechanical integrity.

Classical fin, or extended surface, thermal analysis is based on the Murray-Gardener [5] assumptions, which – along with other assumptions – neglect orthotropy in the fin material and the presence of radial temperature gradients in the fin. While many of these assumptions have been relaxed in subsequent analyses [6-17], including development of two-dimensional fin equations, thermal orthotropy has generally not been specifically addressed in pin fin design.

The present effort focuses on polymer composite cylindrical pin fins with orthotropic thermal conductivity. The paper begins with a brief review of the one-dimensional (1D) and two-dimensional (2D) fin analyses, followed by a comparison of analytical 1D and 2D solutions, and FEM simulations for fins with different radial Biot numbers. The governing heat transfer equation for an orthotropic pin fin is derived and used to delineate the effect of thermal orthotropy in pin fin heat transfer. The impact of thermal orthotropy on air-cooled and water-cooled fins is discussed. Finally, a simplified orthotropic pin fin governing equation is obtained for use in pin fin and heat sink design.

NOMENCLATURE

A	area, m^2
Bi	Biot number, hR/k
h	heat transfer coefficient, W/m^2-K
H	pin fin height, m
J	Bessel function
k	thermal conductivity, W/m-K
k*	conductivity ratio, k_r/k_z
m	fin parameter, $(2h/kR)^{1/2}$
q	heat flow rate, W
q*	heat flow parameter, $q/k\theta R$
R	pin fin radius, m
T	temperature, K
r, z	polar coordinates, m
Subscripts and superscripts	
a	ambient
b	fin base
c	cross section
gm	geometric mean, $(k_r k_z)^{1/2}$
hm	harmonic mean $(2k_r k_z)/(k_r + k_z)$
r	radial
z	axial
‘	correction
0	zero order
1	1st order
Greek symbols	
θ	T_b-T_a
γ	aspect ratio, $\gamma = H/R$
λ	eigenvalues,
Σ	standard deviation
η	fin efficiency

ISOTROPIC PIN FIN MODELS

Literature Review:

The classical solution [5, 6] for one-dimensional heat flow in a cylindrical pin fin, without tip heat loss is given by:

$$q_b = -kA_c\, d\theta/dz\big|_{z=H} = \pi kR^2\theta_b \tanh mH \qquad (1)$$

$$\eta = \tanh mH/mH \qquad (2)$$

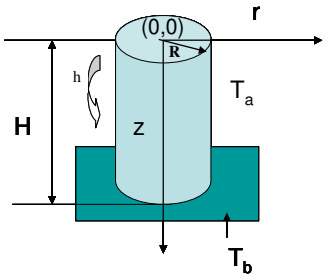

Figure 1: Pin fin coordinates

Equation (1) can be modified [7] to approximate heat flow in a fin with tip loss, by extending the fin height and defining an effective height, H’ as:

$$H' = H + R/2 \qquad (3)$$

A more rigorously derived one-dimensional fin equation with fin tip heat loss, described in [8], takes the form,

$$q_b = \pi\sqrt{2Bi}\left(\frac{\sinh\gamma\sqrt{2Bi} + (Bi/2)^{1/2}\cosh\gamma\sqrt{2Bi}}{\cosh\gamma\sqrt{2Bi} + (Bi/2)^{1/2}\sinh\gamma\sqrt{2Bi}}\right) \qquad (4)$$

In an effort to address two-dimensional behavior in this one-dimensional relation, Aparecido and Cotta [8] proposed a modified radial Biot number, Bi’ that can be inserted into Eq. (4) as,

$$Bi' = 6Bi/(Bi+6) \qquad (5)$$

They then presented evidence that the resulting relation yielded agreement with the 2D equation to within -0.1% for γ, equal to 5, and Bi, equal to1 and up to 14% for γ equal to 5 and Bi equal to 10.

A rigorously derived two-dimensional cylindrical pin fin excess temperature equation takes the form

$$\theta(r,z) = 2\theta_b\sum_{n=1}^{\infty}\frac{\lambda_n J_1(\lambda_n)J_0(\lambda_n\frac{r}{R})}{J_o^{\,2}(\lambda_n)[\lambda_n^{\,2}+Bi^2]}\left[\frac{1+\exp(-2(\lambda_n\frac{z}{R}+\tanh^{-1}(\frac{Bi}{\lambda_n}))}{1+\exp(-2(\lambda_n\gamma+\tanh^{-1}(\frac{Bi}{\lambda_n}))}\right]$$

$$\text{x}\ \exp(-\lambda_n(H-R)/z) \qquad (6)$$

$$\text{Where}\ J_1(\lambda_n) = \frac{Bi}{\lambda_n}J_o(\lambda_n) \qquad (7)$$

The heat transfer rate from the fin base is obtained by differentiating Eq. (6) and finding the value of the first derivative of the excess temperature, θ, at z=H. The heat transfer rate from the fin base is then given as,

$$q_b = -k\theta R q_b^* \quad (8)$$

Where the non-dimensional heat flow parameter, q_b^*, is given as,

$$q_b^* = 4\pi \sum_{n=1}^{\infty} \frac{Bi^2}{\lambda_n[\lambda_n^2 + Bi^2]} \times \frac{[1-\exp(-2[\lambda_n \gamma + \tanh^{-1}(\frac{Bi}{\lambda_n})])]}{[1+\exp(-2[\lambda_n \gamma + \tanh^{-1}(\frac{Bi}{\lambda_n})])]} \quad (9)$$

The non-dimensional pin fin heat flow is seen in Eq. (9) to depend primarily on the radial Biot number and to display a relatively weak dependence on pin fin aspect ratio, as concluded by several authors [8, 14, and 15].

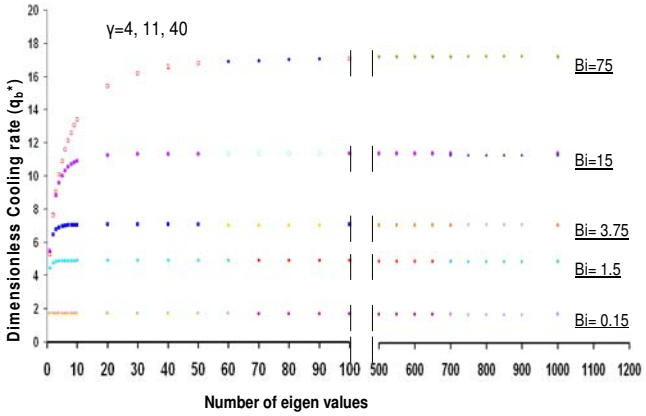

Figure 2: Dependence of non-dimensional isotropic pin fin cooling rate on number of eigen values (red: γ=4, blue: γ=11, green: γ=40)

As may be seen in Fig 2, the number of eigen values required for first decimal convergence of the analytical solution increases from a single term for Bi of 0.15, through 10 for Bi of 15, and to as many as 100 eigen values for Bi of 75, the highest radial Biot number studied. It may also be noted that the convergence of q* is independent of the aspect ratio for a range of γ from 4 to 40.

Isotropic analytical/numerical results:

To further quantify the impact of two-dimensional heat flow in pin fins and establish a valid baseline for understanding the role played by orthotropy in this configuration, a FEM model, using ANSYS 7.1, was developed. The convergence of the FEM-derived pin fin heat transfer rate with the node count is shown in Figure 3 and it reveals that some 30,000 nodes were needed to achieve a "mesh-refined" solution to a first decimal place accuracy for Bi=15 and about 125,000 for a Bi=75, for which the larger temperature gradients necessitate a larger number of nodes to properly capture the temperature field. A comparison of Figs 2 and 3 reveals the fully-converged analytical and FEM results to be in close agreement (0.4%) with each other.

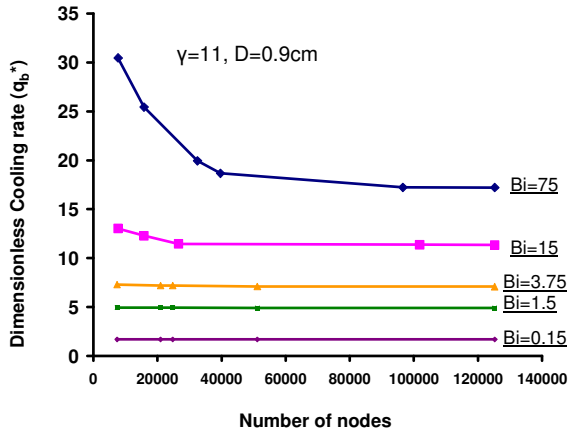

Figure 3: Non-dimensional isotropic pin fin cooling rate – FEM mesh refinement effect

To more clearly display the effect of the radial Biot number on isotropic fin heat transfer, the analytical and numerical results for heat flow in an "extreme" 9mm diameter, 50mm long, pin fin are shown in Figure 4. It is to be noted that the smaller Bi values are obtained with a fin thermal conductivity of 20W/mK and heat transfer coefficients ranging from 10W/m^{2}K (Bi=0.0022) to 5000 W/m^{2}K (Bi= 1.125), while Bi values approaching 75 were obtained with a thermal conductivity of 0.3W/mK, typical of an un-enhanced polymer, and a heat transfer coefficient of 5000 W/m^{2}K, as might be encountered in compact water-cooled heat exchangers [18, 19].

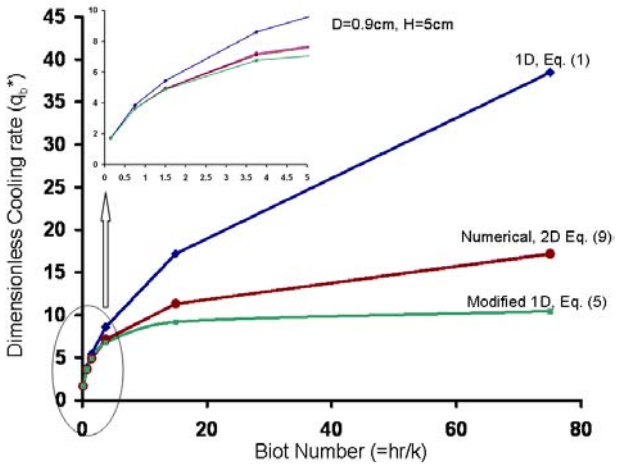

Figure 4: Variation of non-dimensional isotropic pin fin cooling rate with radial Biot number (H=50mm, D=9mm)

Figure 4 makes it clear that while the heat transfer rate from a pin fin can be determined using the classical pin fin equations up to Biot numbers of 0.5 (with less than a 4% discrepancy), the Aparecido and Cotta modified 1D relations [8] extend this agreement up to Biot numbers of 5 (15% accuracy). However, beyond these Biot values the classical 1D formulation over-predicts and the Aparecido and Cotta modified 1D equation under-predicts the pin fin cooling rate. Alternately, the values obtained from the rigorously-derived 2D, isotropic pin fin

equation agree very closely (≤0.2%) with the FEM results up to radial Biot Numbers close to 75.

Implications:

The observed discrepancies at progressively larger Bi derive from the inability of the 1D formulation to accurately capture the temperature gradients that develop in an orthotropic pin fin and that are accentuated by low thermal conductivity, large radius, and high heat transfer coefficients. This behavior can be seen in Fig 5a and Figure 5b that display, side by side, the two dimensional and one dimensional temperature contour plots for a 9mm radius and 50 mm high polymer fin, with a thermal conductivity of 1 W/m-K and a radial Biot number of 0.45. The fin has a constant base temperature of 95 ^{o}C and is exposed to a heat transfer coefficient of 50 W/m^2-K in a 45 ^{o}C ambient temperature. The classical 1D solution, Eq. (1), by assumption, produces isotherms that are parallel to the pin fin base and display no radial component (Fig 5b). However, the more rigorous 2D solution, Eq. (6), results in isotherms that, even at this modest Bi number of 0.45, are radially parabolic (Fig 5a). As a consequence of these different temperature profiles, the 1D solution for the specified pin fin configuration overpredicts the cooling rate (1.34 W) by 3.8% compared to the value predicted by the more rigorous 2D relation (1.29 W).

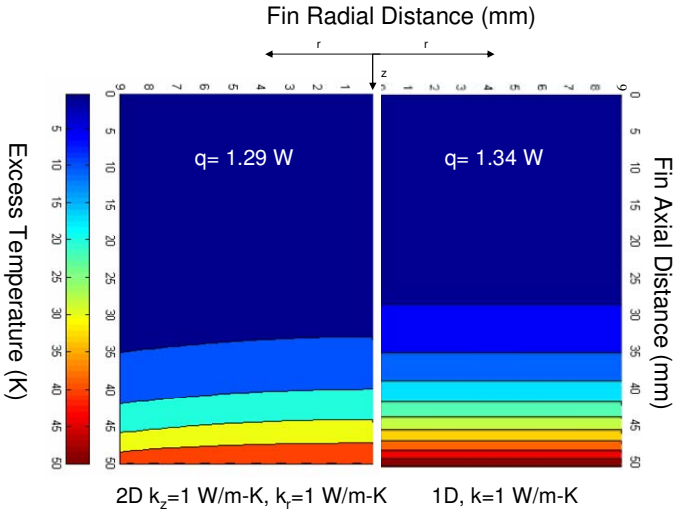

Figure 5: Analytical excess temperature profile for an isotropic low conductivity pin fin (a) 2D temperature field using Eq. (6) (b) 1D temperature field using Eq. (1)

To provide a context for this wide range of Biot numbers, consider a 3.18 x 10^{-6}m^3 (3.18cm^3) polymer pin fin operating at 73% efficiency. When subjected to a typical forced convection heat transfer coefficient of 25W/m^{2}K, an unenhanced polymer pin fin with a thermal conductivity of 0.3 W/m-K will have a 9.75 mm radius and 7.6 mm length, yielding a Bi of 0.81. This same volume and material fin cooled by water, with an 'h' of 1000 W/m^2-K, can be shown to possess a radius of 19.7mm and display a Biot number of 66. Alternatively, the Bi of a 3.18cm^3 fin made of enhanced polymer with a conductivity of 3 W/m-K and cooled by a 25W/m^{2}K heat transfer coefficient is equal to 0.051. It may, therefore, be expected that the performance of unenhanced, isotropic air cooled fins and enhanced water-cooled fins will display some significant departures from the classical predictions. On the other hand, for enhanced polymer fins used in air-cooled applications, it would appear that reasonably accurate results can be obtained using the classical 1D solution for all but the highest heat transfer coefficients.

However, the use of orthotropic polymer composite pin fins, with lower radial thermal conductivity than axial thermal conductivity, can be expected to lead to much larger radial temperature gradients than experienced in isotropic fins and, consequently, to greater deviations from the classical 1D fin solutions. If these newly available composite materials are to be successfully used for fins and heat sinks it is, thus, imperative that the effect of thermal orthotropy be incorporated into the thermal analysis and design of such orthotropic pin fins.

ORTHOTROPIC PIN FIN -DETAILED MODEL

Analysis:

For steady state heat conduction in a radially symmetric, orthotropic fin with no internal heat generation and with $\theta = T - T_a$, the energy equation can be expressed in cylindrical coordinates, as

$$k_r \frac{\partial^2 \theta}{\partial r^2} + k_r \frac{1}{r}\frac{\partial \theta}{\partial r} + k_z \frac{\partial^2 \theta}{\partial z^2} = 0 \qquad (10)$$

Solution of this equation is sought under the following boundary conditions (referring to Figure 1):

a. Symmetric boundary condition at the fin center line:

$$r = 0 \qquad \frac{\partial \theta}{\partial r} = 0 \qquad (11)$$

b. Uniform heat transfer coefficient at the fin tip

$$z=0 \qquad k_z \frac{\partial \theta}{\partial z} = h\theta \qquad (12)$$

c. Uniform heat transfer coefficient at fin surface

$$r = R \qquad -k_r \frac{\partial \theta}{\partial r} = h\theta \qquad (13)$$

d. Fixed fin base excess temperature

$$z=H \qquad \theta = \theta_b \qquad (14)$$

Eq. (10), the governing equation for the fin excess temperature, is homogeneous and the method of separation of variables can be applied. Carrying out the separation of variables and obtaining coefficients using orthogonality of Bessel functions with utilization of the stated boundary conditions in Eqs. (11-14), the radial and axial variation of the pin fin excess temperature, θ(r, z) is found as,

$$\theta(r,z) = 2\theta_b \sum_{n=1}^{\infty} \frac{\lambda_n J_1(\lambda_n) J_o(\lambda_n \frac{r}{R})}{J_o^{\,2}(\lambda_n)[\lambda_n^{\,2} + Bi_r^{\,2}]} \mathrm{X}$$

$$\frac{[1+\exp(-2[\lambda_n (k^*)^{1/2} z/R + \tanh^{-1}(\frac{Bi_{gm}}{\lambda_n})])]}{[1+\exp(-2[\lambda_n (k^*)^{1/2}\gamma + \tanh^{-1}(\frac{Bi_{gm}}{\lambda_n})])]} \exp(-\lambda_n (k^*)^{1/2}(H-z)/R) \qquad (15)$$

Differentiation of Eq. (15) and evaluation of the temperature gradient at z=H, yields the relation for fin heat flow, q_b, as

$$q_b = -4\pi\theta_b R(k_z)^{1/2}\sum_{n=1}^{\infty}$$

$$\frac{Bi_r^{\,2}}{\lambda_n[\lambda_n^{\,2}+Bi_r^{\,2}]}\frac{[1-\exp(-2[\lambda_n\gamma(k^*)^{1/2}+\tanh^{-1}(\frac{Bi_{gm}}{\lambda_n})])]}{[1+\exp(-2[\lambda_n\gamma(k^*)^{1/2}+\tanh^{-1}(\frac{Bi_{gm}}{\lambda_n})])]} \quad (16)$$

The eigen values for both Eqs. (15) and (16) are found by using the boundary condition expressed by Eq. (12) to obtain the following eigen value equation,

$$J_1(\lambda_n) = \frac{Bi_r}{\lambda_n} Jo(\lambda_n) \quad (17)$$

It is to be noted that eliminating the orthotropy contained in Eq. (16) by setting, $k_r = k_z = k$ and, hence $Bi_r = Bi_{gm} = Bi$, and k*=1 reduces Eq. (16), as expected, to Eq. (9), the previously described 2D isotropic pin fin equation. In order to conform to classical form, the exponential terms in Eq. (16) can be converted to hyperbolic tangents, yielding,

$$q_b = -4\pi\theta_b R(k_z)^{1/2}\sum_{n=1}^{\infty} \frac{Bi_r^{\,2}}{\lambda_n[\lambda_n^{\,2}+Bi_r^{\,2}]}$$

$$\text{X}\tanh[\lambda_n\gamma(\frac{k_r}{k_z})^{1/2}+\tanh^{-1}(\frac{Bi_{gm}}{\lambda_n})] \quad (18)$$

ORTHOTROPIC PIN FIN RESULTS

Analytical/Numerical Comparison:

Figure 6 displays a comparison of the analytical and numerical results obtained using ANSYS 7.1 for the heat flow from an orthotropic pin fin, including a total of 99 distinct data points, for three different thermal conductivity ratios, k*=0.015, 0.25, and 1, and radial Biot numbers varying from 0.01-15. The plot clearly indicates very strong agreement (standard deviation, σ, =0.073) between the analytical results Eq. (16) and the simulation results, for the heat transfer rate from a single orthotropic pin fin, with diameter of 9mm and fin height of 50 mm, and an axial thermal conductivity of 20 W/m-K. The heat transfer coefficient ranges from 10 – 5000 W/m^2-K.

Temperature Profile:

The impact of thermal orthotropy can be clearly seen in Figure 7, showing a comparison of the temperature profile for a thermally enhanced, polymer pin fin with an axial thermal conductivity 60 times higher than the 0.3W/mK radial thermal conductivity, in Fig 7a, and a pin fin with an isotropic thermal conductivity of 20W/mK, in Fig 7b. The pin fin in both cases has a 9mm diameter and a 50mm height; the fin base temperature is fixed at 95 ^{o}C in an ambient temperature of 45 ^{o}C, and exposed to a uniform convective heat transfer coefficient of 1000 W/m^2-K. While both images in Figure 7 reveal the two-dimensional character of the temperature profile, the orthotropic isotherms, shown in Figure 7a and reflecting the impact of the low radial conductivity, display a smaller axial gradient near the fin base and a far larger radial temperature gradient than the isotropic isotherms of Figure 7b, throughout the fin volume. As a result of these gradients, which act to lower the surface temperature of the orthotropic fin, at the stated thermal conductivity ratio, the inclusion of orthotropic effects leads to a 33% decrease in the fin heat transfer rate (6.25W vs. 9.28W) relative to what is obtained with the 2D isotropic analysis.

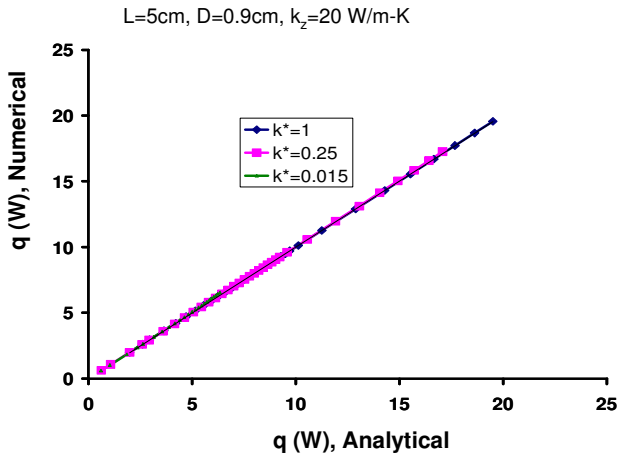

Figure 6: Comparison of analytical and numerical orthotropic pin fin heat transfer rates – various conductivity ratios.

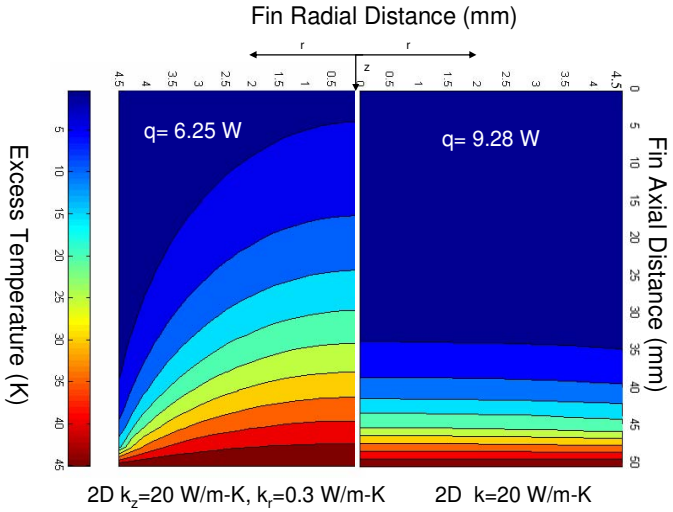

Figure 7: Analytical excess temperature profile for a pin fin (a) Orthotropic 2D - Eq. (15) (b) Isotropic 2D - Eq. (6) (H=50mm, D=9mm, h=1000W/m^{2}K))

Parametric Trends:

In order to more comprehensively explore the thermal behavior of an orthotropic pin fin, attention is now turned to the heat transfer rate of the previously defined pin fin geometry, for the stated boundary conditions and for a broad range of radial and axial thermal conductivities.

Thermal Conductivity: Examination of Eq. 18 suggests that the axial thermal conductivity, which appears outside the summation sign raised to the 0.5 power (as well as in the hyperbolic tangent argument inside the summed eigen valued terms), exerts a more powerful influence on the heat transfer rate than the radial thermal conductivity, which appears only inside the summed eigen valued terms (in the numerator of the Biot number terms and in the hyperbolic tangent argument).

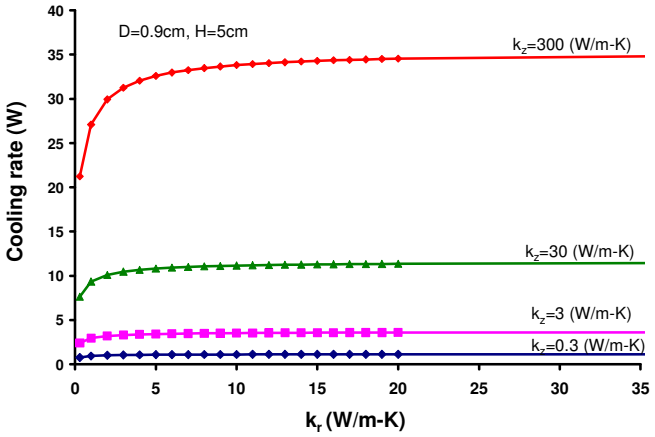

Figure 8: Orthotropic pin fin cooling rate variation with radial and axial thermal conductivity - Eq. (18)

Figure 8 reveals this behavior, showing the axial thermal conductivity to exert the dominant effect on the heat transfer rate from a 9mm diameter, 50mm high pin fin, which follows an approximately square root dependence on k_z, as the axial thermal conductivity increases from 0.3 to 300W/mK. The relatively weaker, though more complex, cooling rate dependence on the radial thermal conductivity is seen in Figure 8 to experience a linear rise at relatively small values of k_r, followed by a gentle asymptotic rise over a large range of k_r values, for each value of k_z. Despite the complex functional dependence of q_b on k_r in Eq. 18, this hyperbolic-tangent-like behavior may well reflect the presence of k_r in the argument of the hyperbolic tangent function in the summation of eigen valued terms. For the conditions studied numerically, the asymptotic domain appears to begin at progressively higher k_r values as the axial thermal conductivity value increases. Thus for k_z=0.3W/m-K the asymptotic transition occurs in the vicinity of k_r=1W/m-K, while for an axial thermal conductivity of 30 W/m-K, the asymptotic zone begins at k_r=10W/m-K.

Figure 9 depicts the variation of the pin fin cooling rate with fin height, for a fixed axial thermal conductivity of 20 W/m-K in an isothermal medium with a fixed heat transfer coefficient of 1000W/m^2-K. Increasing the thermal conductivity ratio (by increasing the radial thermal conductivity) is seen to have a strong effect on the cooling rate for values of k* below unity and a progressively weaker effect for larger values of k*. As the conductivity ratio increases above unity, the radial temperature gradients diminish and fin performance asymptotically approaches the heat transfer rates obtained from the classical 1D relation.

Fin height: Interestingly, the variation with height - at conductivity ratios of unity as well as higher and lower values – mimics the asymptotic approach (typically hyperbolic tangent variation) to the maximum fin heat transfer rate found in the classical 1-D pin fin solution. This behavior is reflected in the appearance of the fin height in the argument of the hyperbolic tangent inside the eigen valued summation in Eq. 18. Thus, as with isotropic fins, there is not much to be gained in heat transfer by increasing pin fin height beyond a relatively modest value, which yields the near-maximum heat transfer rate. For the conditions examined, as shown in Figure 9, this fin height is a very weak function of the radial thermal conductivity for a range of fin aspect ratios from 0.2 to approximately 200. This conclusion has been further verified by performing similar analyses for heat transfer coefficient values of 10 and 100 W/m^2-K shown in Fig. 9.

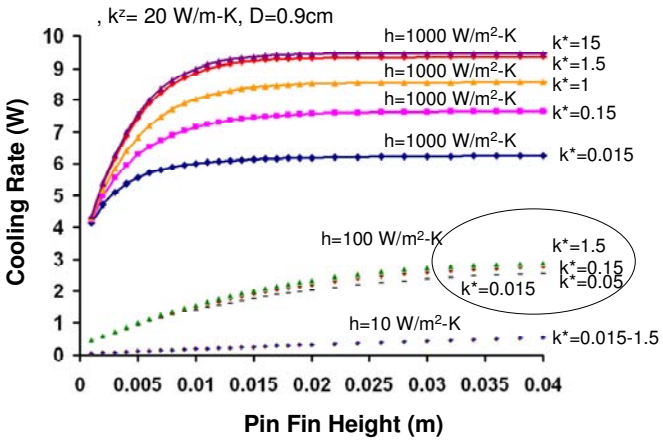

Figure 9: Orthotropic pin fin cooling rate variation with fin height - Eq. (18)

Conductivity ratios: The more explicit effect of the thermal conductivity ratio on the pin fin cooling rate is depicted in Figure 10 for a polymer composite pin fin, with a fixed diameter of 9mm and a fin height of 50mm, and various heat transfer coefficients. In natural convection, with heat transfer coefficient values of approximately 10W/m^2-K, the cooling rate stays constant over a wide range of thermal conductivity ratios, indicating negligible thermal orthotropy effects. However, for high heat transfer coefficient values (500-5000W/m^{2}K), attained typically in liquid cooled systems, the cooling rate increases significantly with the radial thermal conductivity and vice versa.

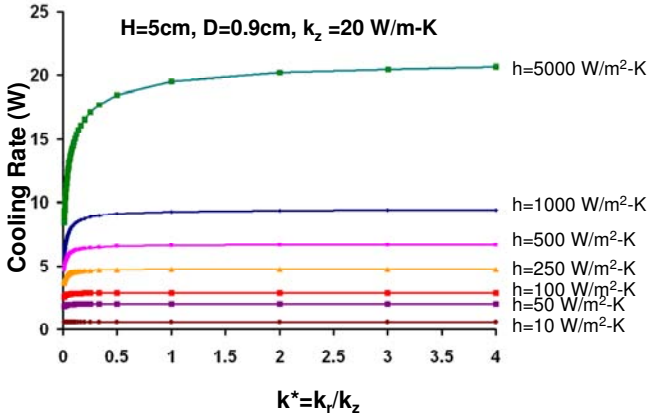

Figure 10: Orthotropic pin fin cooling rate variation with thermal anisotropy - Eq. (18)

Effective conductivity: Given the relatively modest effect of the conductivity ratio on pin fin heat transfer, it is tempting to explore the potential for capturing the orthotropic effect through the use of an "effective" thermal conductivity in the 1D relation. Figure 11 displays the cooling rates obtained using Eq. 1 for a single orthotropic pin fin of diameter 9mm, fin height

50mm, and a conductivity ratio of 60, subjected to a range of heat transfer coefficients and using several "effective" thermal conductivity values.

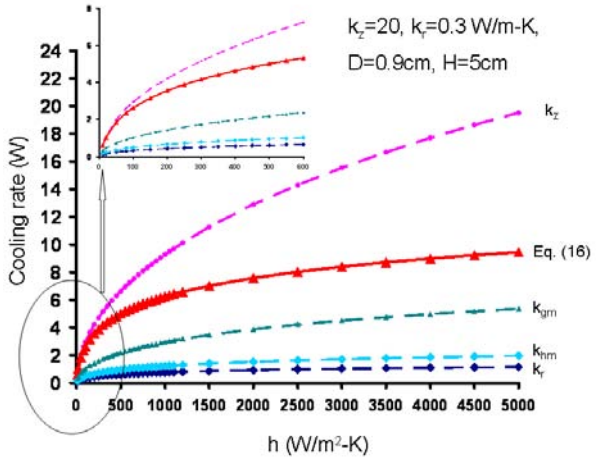

Figure 11: Orthotropic pin fin cooling rate based on 1D model with effective thermal conductivities

Examining Fig. 11, it is to be noted that the use of an effective thermal conductivity value based on the axial conductivity alone, as well as on the harmonic mean (0.6 W/m-K) or geometric mean (2.45 W/m-K) of k_r and k_z, and on the radial conductivity alone, is incapable of predicting – even approximately – the cooling rate of the orthotropic fin over the broad range of heat transfer coefficients studied. However, for air-cooling heat transfer coefficients up to approximately 70 W/m^2-K, use of the axial thermal conductivity does provide a predictive accuracy to within 8%.

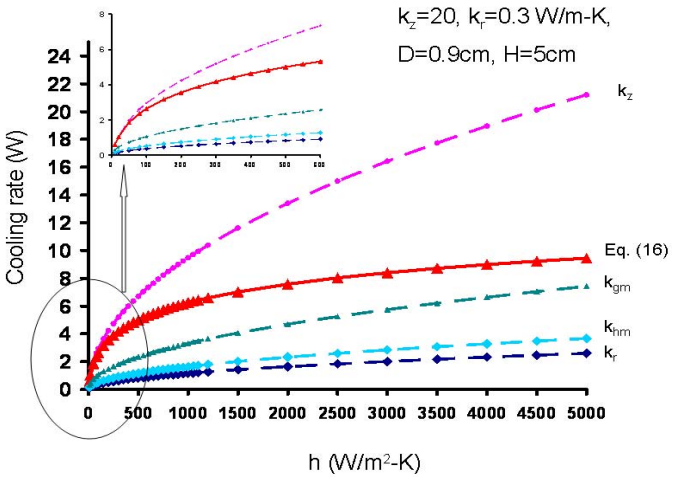

Figure 12: Orthotropic pin fin cooling rate based on isotropic 2D relation with effective thermal conductivities - Eq. (9)

Moreover, even when the two-dimensional isotropic relation Eq. (9) is used, it is seen in Figure 12 that none of the effective single thermal conductivity values can be used to accurately predicts the orthotropic pin fin cooling rate, for heat transfer coefficients above 70 W/m^2-K For h values of about 80W/m^2-K the 2D isotropic prediction shows an approximately 10% discrepancy, which grows to 110% at 1500 W/m^2-K, relative to the 2D orthotropic results using Eq. (18).

APPROXIMATE ORTHOTROPIC PIN FIN RELATIONS

For typical pin fin geometry, fin tip area is significantly less than the total wetted area. Therefore it is possible to approximate fin heat transfer by assuming negligible heat transfer from the pin fin tip. Setting $\partial\theta/\partial z$ to zero in Eq. (12) at the fin tip, and repeating the analysis described above, the total heat transfer rate from the lateral surface area of a tip-insulated pin fin is found to be expressible as

$$q_b = -4\pi k_z \theta_b R (k^*)^{1/2} \sum_{n=1}^{100} \frac{Bi_r^2}{\lambda_n[\lambda_n^2 + Bi_r^2]} \tanh\lambda_n \left(\frac{k_r}{k_z}\right)^{1/2} \gamma) \qquad (19)$$

It is possible to modify Eq. (19) and include fin tip heat loss for increasing accuracy over larger aspect ratio range by adding one fourth of the pin diameter to pin fin height [7].

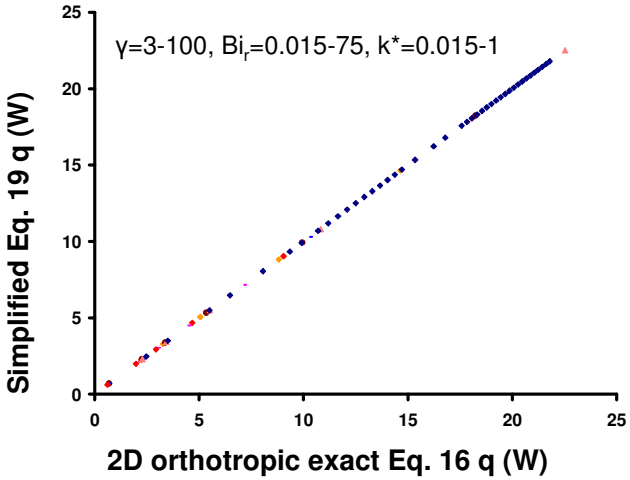

Figure 13: Comparison of orthotropic cooling rates using insulated tip pin fin equation (Eq. (19))

Fig 13 displays a comparison between the orthotropic pin fin cooling rates, calculated using Eq. (19) with modified pin fin height, spanning aspect ratios (H/R) of 3-100, thermal conductivity ratios (k*) from 0.015-1, and heat transfer coefficients ranging from 10W/m^2-K to 5000 W/m^2-K, for a total of 547 different cases. The discrepancy observed between the results obtained with Eq. (19) and Eq. (16) respectively was 3.7%, for the case with lowest fin aspect ratio of 3, the thermal conductivity ratio of 0.05, and the highest considered heat transfer coefficient of 5000 W/m^2-K. As anticipated, the error associated with the use of the far simpler Eq. (19) decreases monotonically with increasing aspect ratios and conductivity ratios**.** Using Eq. (19) without this tip loss correction exceeds a 10% discrepancy at a fin aspect ratio of 4 and the thermal conductivity ratio of 0.05. Using Eq. (19) with corrected fin height 10% can be extended to aspect ratio as low as 2.

Slender (High aspect ratio) fins

Further simplification of the insulated tip orthotropic pin fin relation can be obtained by observing that the exponential terms in Eq. (20) become negligibly small for fins with aspect ratios greater than 20. The heat transfer rate from such pin fins can be expressed in the form of Eq. (20), i.e.

$$q = -4\pi k_z \theta_b R(\frac{k_r}{k_z})^{1/2} \sum_{n=1}^{100} \frac{Bi_r^{\,2}}{\lambda_n[\lambda_n^{\,2} + Bi_r^{\,2}]} \qquad (20)$$

Figure 14 displays a comparison between the orthotropic pin fin cooling rates, calculated using simplified Eq. (20) and exact Eq. (16), spanning fin aspect ratios (H/R) of 20-100, thermal conductivity ratios (k*) from 0.015-1, and heat transfer coefficients ranging from 10 W/m^2-K to 5000 W/m^2-K, for a total of 373 different cases. The highest discrepancy observed between the results obtained with Eq. (20) and Eq. (16), respectively, was 0.12%, for the case with the lowest fin aspect ratio of 20, lowest thermal conductivity ratio of 0.015 and lowest heat transfer coefficient of 10 W/m^2-K. As the fin aspect ratio increases beyond 20, agreement increases between the Eq. (20) and Eq. (16) predictions.

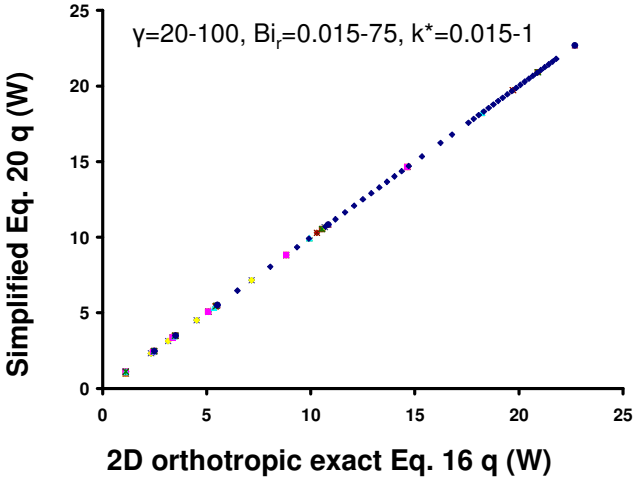

Figure 14: Comparison of orthotropic pin fin cooling rate - simplified and orthotropic equations - Eq. 16 and 20

CONCLUSIONS

The growing interest in thermally-enhanced, polymer composite fins has motivated this development of an analytical equation for heat transfer from a cylindrical pin fin with orthotropic thermal conductivity. The resulting relation was numerically validated over a broad parametric range, including fin thermal conductivity ratios of 0.015-15, aspect ratios of 4-100, and radial Biot numbers of 0.0056-75. For the range studied, the impact of orthotropy on the pin fin heat transfer rate is found to increase with the radial Biot number and to decrease with the thermal conductivity ratio (radial/axial) and fin aspect ratio.

For polymer composite pin fins, cooled by typical natural and forced convection air flows, yielding fin Biot numbers below 0.5,orthotropic effects were found to be limited to just several percent corrections in fin heat transfer rates. In more aggressive air cooling scenarios, where fin Bi can exceed unity, the proposed equation provides significantly more accurate results than the classical 1D relation.

For water cooled fins, where heat transfer coefficients can approach and exceed 1000 W/m^2-K and efficient fins tend to be thicker, large radial Biot number are attained and orthotropic thermal conductivity effects are very prominent. Approximate orthotropic pin fin solutions for typical (>3) and high aspect ratio (>20) pin fins were also found, yielding agreement to exact closed form equation within 3.7% and 0.12%, respectively, across the appropriately restricted parametric range.

REFERENCES

[1] Zweben, C., Emerging high-volume commercial applications for thermally conductive carbon fibers, sixth international business conference on the global outlook for carbon fiber, San Diego, California, USA, November 5 – 7, 2003.

[2] Gary Shives et. al., Comparative thermal performance evaluation of graphite/epoxy fin heat sinks, Proceedings, ITHERM 2004, pp. 410-417.

[3] M. J. Biercuk, M. C. Laguno, M. Radosavljevic, J. K. Hyun, A. T. Johnsond, and J. E. Fischer, Carbon nanotube composites for thermal management, Applied Physics Letters, 80, 2002, pp. 2767-2769.

[4] Bahadur, R., and Bar-Cohen, A., Thermal design and optimization of staggered polymer pin fin natural convection heat sinks, I.E.E.E Transactions on components and packaging technology, June 2005 future publications.

[5] Gardner, K. A., Efficiency of extended surfaces, Trans. ASME, vol. 67, 1945, pp. 621-631. .

[6] Kern, D. A., and Kraus, A. D., Extended surface heat transfer, McGraw-Hill, New York, 1972, pp. 114-115.

[7] Harper, D. R., and Brown, W. B., Mathematical equations for heat conduction in the fins in air cooled engines, NACA technical report, p. 188, 1922.

[8] Aparecido, J. B., Cotta, R. M., Improved one dimensional fin solutions, Heat transfer engineering, vol. 11, 1, pp 49-59.

[9] Kraus, A.D., Aziz, A., Welty, J., Extended Surface heat transfer, Wiley, New York, (2001), pp. 723-724.

[10] Levitsky, M. J., The criterion for the validity of the fin approximation, Int. J. Heat M. Transfer, 15, 1960, pp. 1960-63.

[11] Ozisik, M., N., Heat conduction, 2nd ed. Wiley, New York, (1993).

[12] Poulikakos D., Conduction heat transfer, Prentice Hall, Englewood Cliffs, NJ, 1994.

[13] Gebhart, B., Heat Conduction and mass diffusion, McGraw-Hill, New York, 1993.

[14] Irey, R.K., Error in one dimensional fin solution, J. Heat Transfer, 90, 1968, pp. 175-176.

[15] Lau, W., and Tan, C. W., Errors in one dimensional heat transfer analysis in straight and annular fins, J. Heat Transfer, 95, November 1973, pp. 549-551.

[16] Mikhailov, M.D., and Ozisik, M.N., Unified analysis and solutions of heat and mass diffusion, John Wiley, 1984.

[17] Aziz, A., and Nguyen, H., Two dimensional performance of conducting-radiating fins of different profile shapes, Waerme and Stoffuebertrag, 28, 1993, pp. 481.

[18] Davidson, J.H., et al. Are plastic heat exchangers feasible for solar water heaters? Part I: A review of codes and standards and commercial products. in 1999 ASME International Solar Energy Conference. 1999. Maui, Hawaii.

[19] Liu, W., et al. Thermal and economic analysis of plastic heat exchangers for solar heating in solar 99, the 1999 American Solar Energy Conference. 1999, Portland, OR.

[20] Weber, E., Development and modeling of thermally conductive polymer/carbon composites, PhD thesis in chemical engineering at Michigan Technology University, 1999.